nature COMMUNICATIONS

ARTICLE

DOI: 10.1038/s41467-018-05880-4 OPEN

Selective conversion of CO_2 and H_2 into aromatics

Youming Ni[1,2], Zhiyang Chen[1,2,3], Yi Fu[1,2,3], Yong Liu[1,2], Wenliang Zhu[1,2] & Zhongmin Liu[1,2]

Transformation of greenhouse gas CO_2 and renewable H_2 into fuels and commodity chemicals is recognized as a promising route to store fluctuating renewable energy. Although several C_1 chemicals, olefins, and gasoline have been successfully synthesized by CO_2 hydrogenation, selective conversion of CO_2 and H_2 into aromatics is still challenging due to the high unsaturation degree and complex structures of aromatics. Here we report a composite catalyst of $ZnAlO_x$ and H-ZSM-5 which yields high aromatics selectivity (73.9%) with extremely low CH_4 selectivity (0.4%) among the carbon products without CO. Methanol and dimethyl ether, which are synthesized by hydrogenation of formate species formed on $ZnAlO_x$ surface, are transmitted to H-ZSM-5 and subsequently converted into olefins and finally aromatics. Furthermore, 58.1% *p*-xylene in xylenes is achieved over the composite catalyst containing Si-H-ZSM-5. $ZnAlO_x$&H-ZSM-5 suggests a promising application in manufacturing aromatics from CO_2 and H_2.

[1] National Engineering Laboratory for Methanol to Olefins, Dalian Institute of Chemical Physics, Chinese Academy of Sciences, P. O. Box 110 116023 Dalian, People's Republic of China. [2] Dalian National Laboratory for Clean Energy, Dalian Institute of Chemical Physics, Chinese Academy of Sciences, Dalian 116023, People's Republic of China. [3] University of Chinese Academy of Sciences, 100049 Beijing, People's Republic of China. Correspondence and requests for materials should be addressed to W.Z. (email: wlzhu@dicp.ac.cn) or to Z.L. (email: liuzm@dicp.ac.cn)

The utilization of fossil resources such as coal, oil, and natural gas has brought us unprecedented economy and social development in the past two centuries[1], however, continuously increasing the emissions of greenhouse gas CO_2 is threatening our living environment. The renewable energy resources (for example, solar, tidal, wind and biomass) can generate abundant power, but low-efficiency and fluctuating nature limits their widespread applications[2]. These problems above could be effectively overcome via CO_2 hydrogenation to fuels (e.g., gasoline) and commodity chemicals (e.g., methanol, olefins and aromatics) because hydrogen can be acquired from the clean electricity[3–6].

Considering that CO_2 ($\Delta_f G^o = -396\ kJ\ mol^{-1}$) is a chemical inert molecular[3], CO_2 hydrogenation reactions are generally operated under high pressure and hydrogen content over reductive metal catalysts so as to improve the conversion efficiency. Nowadays, C_1 chemicals such as methanol (MeOH), dimethyl ether (DME), formic acid (HCOOH), methane (CH_4), and carbon monoxide (CO) have been selectively synthesized under above conditions[3,4,6,7]. However, production of C_{2+} hydrocarbons such as olefins and liquid fuels from CO_2 are not easy because of high kinetic barriers for C–C coupling[6,8]. In the earlier studies, combination of reverse-water-gas-shift (RWGS, $CO_2 + H_2 \rightarrow CO + H_2O$) and Fischer–Tropsch (FT, $CO + H_2 \rightarrow C_nH_m$) synthesis reactions was considered as a promising method to generate long-chain hydrocarbons from CO_2[2,9]. Nevertheless, due to the restriction of Anderson–Schulz–Flory (ASF) distribution[10,11], the selectivity of C_2–C_4 and gasoline fraction hydrocarbons does not exceed 58% and 48%[12,13], respectively. More recently, high selective olefins or gasoline has been achieved from CO_2 hydrogenation via utilization of oxide/zeolite bifunctional catalysts which have been successfully applied in syngas-to-olefins (STO) or aromatics (STA) reactions[14–20]. Some typical results are as follows: In−Zr oxide, $ZnGa_2O_4$ or ZnO-ZrO_2 combined with SAPO-34 zeolites achieved more than 80% C_2–C_4 olefins[21–23], meanwhile, In_2O_3 or Na-Fe_3O_4 coupled with H-ZSM-5 zeolites reached to approximately 80% gasoline-range hydrocarbons[24,25]. Because metal catalysts or the Brønsted acid sites of the zeolites can catalyze hydrogenation reactions[26,27], it is challenging to synthesize aromatics with high unsaturation degree and complex structures under conditions of high H_2 content. Up to now, there are no reports on the highly selective conversion of CO_2 and H_2 into aromatics.

Here, we report a composite catalyst made by nano-scaled spinel structural $ZnAlO_x$ oxide and H-ZSM-5 zeolite ($ZnAlO_x$&H-ZSM-5), which exhibits 73.9% aromatics selectivity with only 0.4% CH_4 selectivity among the carbon products without CO in CO_2 hydrogenation reaction. RWGS reaction is largely suppressed by increasing H_2/CO_2 ratio or introducing CO. 58.1% *p*-xylene in xylenes is achieved over the composite catalyst containing Si-H-ZSM-5. Reaction mechanism and the causes of excellent aromatization performance are also explored.

Results and Discussion

Catalytic results. CO_2 hydrogenation reactions were conducted over $ZnAlO_x$&H-ZSM-5 under reaction conditions of $H_2/CO_2/Ar = 3/1/0.2$, pressure 3.0 MPa, and 593 K. The effects of space velocity on CO_2 conversion and product selectivity are shown in Fig. 1a. It is surprising to find that the selectivity of aromatics among the carbon products without CO reaches as high as 73.9% with 9.1% CO_2 conversion and 57.4% CO selectivity at space velocity = 2000 ml g^{-1} h^{-1}. This aromatics selectivity is much higher than the about 40% obtained over Na-Fe_3O_4/H-ZSM-5[25] or 14.6% acquired over In_2O_3/H-ZSM-5[24], respectively. Besides that, the liquid (or gasoline-range) hydrocarbons including C_{5+} and aromatics (excluding CO) run up to 80.3% along with merely 0.4% CH_4. As the space velocity substantially rises to 10,000 ml g^{-1} h^{-1}, the aromatics selectivity only slightly decreases to 56.9%. This result is quite different from STA reactions, which were often operated at the GHSV <1500 ml g^{-1} h^{-1} so as to peruse high aromatics selectivity[19,20]. It also can be seen from Fig. 1a that MeOH, DME and C_{2-4} olefins are progressively climbing with the space velocity growing, which suggests that these byproducts might be acted as the intermediates for aromatization. The CO_2 hydrogenation behaviors of various catalysts are compared in Fig.1b. ZnO exhibits 98.2% MeOH selectivity (excluding CO) with 2.6% CO_2 conversion and 63.5% CO selectivity. After mixed with H-ZSM-5, only 29.7% aromatics selectivity was achieved. Compared to ZnO, $ZnAlO_x$ shows a higher CO_2 conversion (5.1%) but lower CO selectivity (54.9%). The DME and MeOH selectivity is up to 42.8% and 56.2% over $ZnAlO_x$, respectively. It implies that AlO_x component is acted as the active site for MeOH dehydration. In contrast with the composite catalyst ZnO&H-ZSM-5, the composite catalyst $ZnAlO_x$&H-ZSM-5 shows a much better aromatization performance, over which 66.2% aromatic selectivity is obtained under the same reaction conditions. As shown in Fig. 1b, although the CO_2 conversion and liquid hydrocarbons selectivity are approximate, the aromatics selectivity for $ZnAlO_x$&H-ZSM-5 prepared by two components grinding in an agate mortar is 12.4% higher than $ZnAlO_x$ + H-ZSM-5 prepared by the granules of two components mixing. It is apparent that the proximity of oxides and zeolites for the former catalyst is better than the latter one. It means that the closer proximity favors the selective generation of aromatics. As a comparison, the dual-bed configuration catalyst $ZnAlO_x$/H-ZSM-5 with H-ZSM-5 downstream from the $ZnAlO_x$ provided the poorest behavior with 17.9% aromatics selectivity. The effect of reaction temperature on the CO_2 hydrogenation over $ZnAlO_x$&H-ZSM-5 is investigated. Although raising temperature can increase the CO_2 conversion, the ability of aromatization is considerably weakened (Supplementary Fig. 1). The optimized weight ratio of oxide/zeolite is 1:1 (Supplementary Fig. 2). We also studied the CO_2 hydrogenation over the mixture of conventional methanol synthesis catalyst $CuZnAlO_x$ and H-ZSM-5. As shown in Supplementary Fig. 3, the RWGS reaction is predominant, which leads to more than 95% CO selectivity. According to the conditions for CO_2 hydrogenation, CO hydrogenation over $ZnAlO_x$&H-ZSM-5 was investigated at $H_2/CO/Ar = 3/1/0.2$, space velocity = 6000 ml g^{-1} h^{-1}, pressure 3.0 MPa, and 593 K. As depicted in Supplementary Fig. 4, the aromatics selectivity (excluding CO_2) is only 12.8% with 4.7% CO conversion. It implies that the excellent aromatization behavior of $ZnAlO_x$&H-ZSM-5 in CO_2 hydrogenation is not related to self-promotion mechanism of CO reported by Cheng et al.[19].

Catalytic stability. The catalytic stability of $ZnAlO_x$&H-ZSM-5 in CO_2 hydrogenation reaction was studied. It is apparent from Fig. 2 that the composite catalyst delivers a good stability in a 100 h test. The CO_2 conversion, liquid hydrocarbons, and CH_4 selectivity among the carbon products without CO levels off at around 5.4, 74.0, and 0.5% after 50 h on stream. Although the aromatics selectivity is slightly decreased from 72.0% in the initial state to 66.0% after 100 h on stream, the formation rate of aromatics can keep about 15 mg g^{-1} h^{-1} because the CO selectivity progressively declines.

Selectivity optimization. In order to improve the efficiency for CO_2 hydrogenation to valuable hydrocarbons such as aromatics, light olefins and gasoline, the RWGS reaction should be suppressed as much as possible. It is very interesting to find from Fig. 3a that as the H_2/CO_2 ratio rises from 3/1 to 9/1, the CO_2

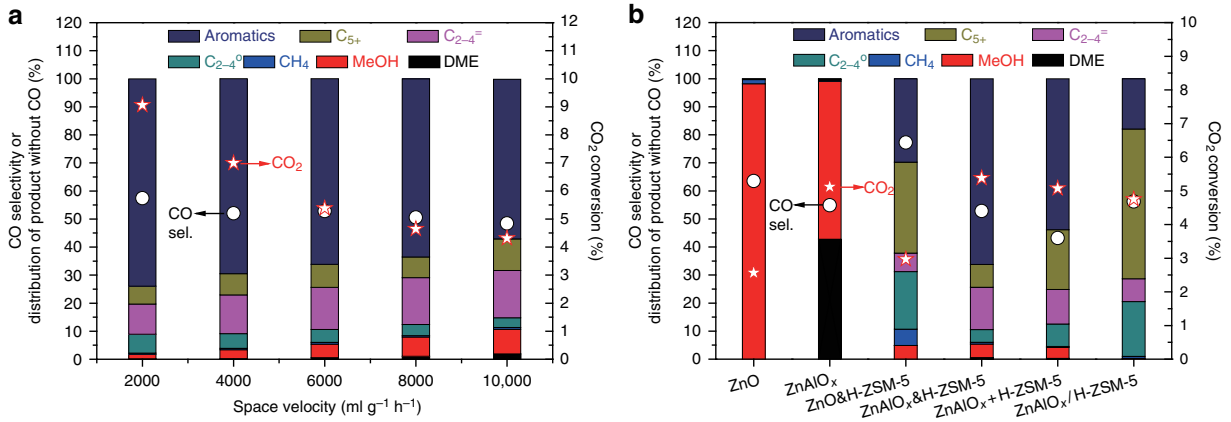

Fig. 1 Catalytic performance for CO_2 hydrogenation. **a** The effect of space velocity over $ZnAlO_x$&H-ZSM-5. Reaction conditions: 593 K, 3.0 MPa, $H_2/CO_2/Ar = 3/1/0.2$. **b** Comparisons of the CO_2 conversion and product selectivity over various catalysts. Reaction conditions: Space velocity = 12,000 (for ZnO and $ZnAlO_x$) or 6000 (for composite catalysts) ml g^{-1} h^{-1}, 3.0 MPa, 593 K, $H_2/CO_2/Ar = 3/1/0.2$. Note that the C_{5+} excludes aromatics. $C_{2-4}^{=}$ and C_{2-4}^{o} refer to C_2–C_4 olefins and paraffins, respectively; $ZnAlO_x$&H-ZSM-5 prepared by grinding; $ZnAlO_x$ + H-ZSM-5 prepared by granules mixing; $ZnAlO_x$/H-ZSM-5 denoted as dual-bed catalysts

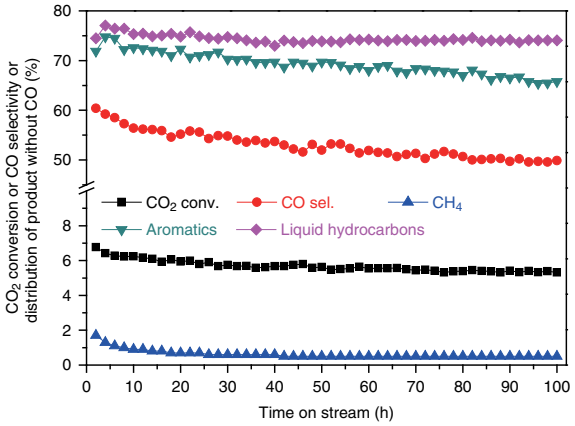

Fig. 2 The stability test for CO_2 hydrogenation over $ZnAlO_x$&H-ZSM-5. Reaction conditions: Space velocity = 6000 ml g^{-1} h^{-1}, 3.0 MPa, 593 K, $H_2/CO_2/Ar = 3/1/0.2$. Note that the liquid hydrocarbons include aromatics

conversion is dramatically increased from 5.8 to 15.7% with the CO selectivity sharply decreasing from 56.9 to 28.7%. It means that the generated CO can be further converted by hydrogenation in the high H_2/CO_2 ratio. Although raising H_2/CO_2 ratio can slightly decrease aromatics selectivity, their formation rate keeps growing. Further increasing H_2/CO_2 ratio to 15/1 leads to a decline in aromatization rate. Moreover, the liquid hydrocarbons are not sensitive to H_2/CO_2 ratio. As shown in Fig. 3b, another effective method to weaken RWGS reaction is adding CO into the mixture gas of CO_2 and H_2. The CO selectivity is nearly monotonically decreasing with CO/CO_2 ratio increasing and as low as 12.6% at CO/CO_2 ratio = 1.8/1, nevertheless, the aromatics or liquid hydrocarbons selectivity is slightly influenced after CO introduction. As known, RWGS is a typical equilibrium reaction[4]. Therefore, introduction product CO does not benefit the formation of itself. These results above are vital to applications. On the one hand, the source of feed gas is more extensive because its composition can be adjusted in a wide range; on the other hand, the product CO can be recycled and accumulated so as to practically depress the RWGS reaction. As presented in Fig. 3c, aromatics with 9 to 10 carbons are predominant over $ZnAlO_x$&H-ZSM-5. We tried to optimize the distributions of aromatics by using Si-H-ZSM-5 made by tetraethoxysilane (TEOS) modification. Compared to $ZnAlO_x$&H-ZSM-5, $ZnAlO_x$&Si-H-ZSM-5 obviously produces more toluene (2.7%) and xylenes (16.8%) (Fig. 3c). Moreover, 58.1% *p*-xylene in xylenes, 25.3% ethylene and 11.9% propylene (excluding CO) along with little C_{1-3} alkanes are obtained over $ZnAlO_x$&Si-H-ZSM-5 (Fig. 3c and Supplementary Fig. 5). The catalytic behavior for $ZnAlO_x$&Si-H-ZSM-5 would be interesting to industry, because ethylene, propylene and *p*-xylene are the most important commodity hydrocarbon chemicals.

Structural characterization. Figure 4a shows the X-ray diffraction (XRD) patterns of $ZnAlO_x$ oxide. The reflection peaks of $ZnAlO_x$ can be approximately assigned to cubic $ZnAl_2O_4$ gahnite[28] (JCPDS 05-0669, Supplementary Fig. 6). The reflection peaks of ZnO (Supplementary Fig. 7) are hardly detectable for $ZnAlO_x$. The Field-emission scanning electron microscopy (SEM) image (Supplementary Fig. 8) shows that the morphology of $ZnAlO_x$ is porous and made by small particles. The BET surface area of $ZnAlO_x$ (Supplementary Table 1) is up to 151.0 m^2 g^{-1}, which is much higher than ZnO (11.9 m^2 g^{-1}). High-resolution transmission electron microscopy (TEM) image in Fig. 4b gives us the fact that the $ZnAlO_x$ sample consists of a lot of tiny nanoparticles with the sizes of <10 nm. Moreover, the lattice spaces of 0.28 and 0.45 nm which respectively correspond to the (220) and (111) planes of cubic $ZnAl_2O_4$ further confirm the spinel structure of $ZnAlO_x$[28]. The element distribution analysis (Supplementary Fig. 9) shows that the Zn, Al, and O are uniformly dispersed. As presented in Supplementary Fig. 10, the ZnO sample in this study is consisted of about 100 nm nanoparticles with a clear lattice space. The H-ZSM-5 zeolite embraces a typical nano-sized MFI structure (Supplementary Fig. 11). The acidcontent of H-ZSM-5 is 1.3 times as high as Si-H-ZSM-5 (Supplementary Table 2). The temperature-programmed reduction (TPR) results in Fig. 4c and Supplementary Table 3 show that both of $ZnAlO_x$ and ZnO can be hardly reduced by H_2 below 700 K and <7% zinc oxides might be reduced to their metal phase above 1000 K. As known, Zn^{2+} cannot be reduced by H_2 due to the positive free Gibbs energy[29]. However, the reduction may proceed if H_2 is split into hydrogen atoms or alloy phase with other metals like Cu is formed[30]. Furthermore, the spinel structure of $ZnAlO_x$ has been proved to be more durable under H_2 reduction[31]. As a result, we consider that it is not zinc metal but Zn^{2+} in $ZnAlO_x$

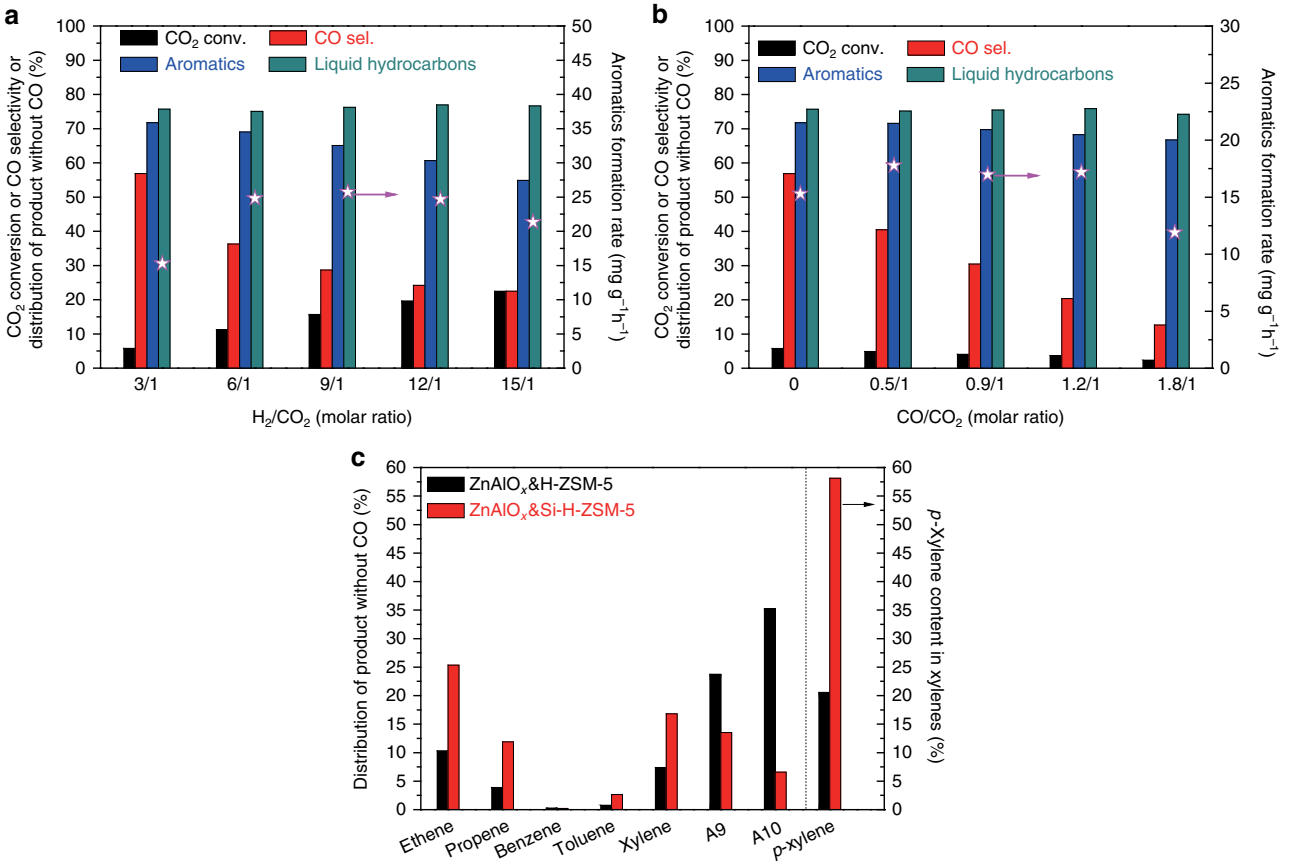

Fig. 3 The results of selectivity optimization for CO_2 hydrogenation. **a** The effect of H_2/CO_2 ratio over $ZnAlO_x$&H-ZSM-5. Reaction conditions: Space velocity = 6000 ml g^{-1} h^{-1}, 3.0 MPa, 593 K. **b** The effect of CO introduction over $ZnAlO_x$&H-ZSM-5. Reaction conditions: catalyst weight = 667 mg, 3.0 MPa, 593 K, inlet gas containing 66.7 ml min^{-1} mixed gas ($H_2/CO_2/Ar$ = 3/1/0.2) and 0–26.6 ml min^{-1} CO. **c** Comparisons of catalytic behaviors over $ZnAlO_x$&H-ZSM-5 and $ZnAlO_x$&Si-H-ZSM-5. Reaction conditions: Space velocity = 6000 ml g^{-1} h^{-1}, 3.0 MPa, 593 K, $H_2/CO_2/Ar$ = 3/1/0.2. A9 and A10 are representative of aromatics containing 9 and 10 carbon atoms, respectively

activates CO_2 hydrogenation reactions in this study. For a long time, the debate about the role of zinc species in industrial Cu/ZnO/Al_2O_3 catalysts for methanol synthesis has always existed. ZnO in Cu/ZnO/Al_2O_3 was not reckoned as catalytic centers but structural promoter or others[32,33]. However, our results prove that in the absence of Cu species, $ZnAlO_x$ can also convert CO_2 into MeOH and derived DME. The FT-IR spectra of catalysts after 2,6-di-tert-butyl-pyridine absorption (DTBPy-FTIR) are exhibited in Fig. 4d. DTBPy-FTIR was usually utilized to investigate the external surface Brønsted acid sites because the kinetic diameter (10.5 Angstrom) of DTBPy is larger than the pore opening (5.5 Angstrom) of H-ZSM-5. The characteristic bands at 3365, 1614 and 1531 cm^{-1} are attributed to the DTBPy adsorbed on the external surface Brønsted acid sites of H-ZSM-5 zeolite. The negative band at 3616 cm^{-1} is assigned to the decrease of bridging hydroxyls on the external surface[34]. Surprisingly, these typical bands almost disappeared for the composite catalyst $ZnAlO_x$&H-ZSM-5. It indicates that external Brønsted acid of H-ZSM-5 can be shielded by $ZnAlO_x$ after mixing, grinding and pressing under high pressure. The external Brønsted acid has no ability to aromatization but can promote the hydrogenation of unsaturated hydrocarbons to paraffins[15,26,27], which is detrimental to the aromatics selectivity. The aromatics or C_{2-4} olefins selectivity follows the order $ZnAlO_x$&H-ZSM-5 > $ZnAlO_x$ + H-ZSM-5 > $ZnAlO_x$/H-ZSM-5 (Fig. 1b), whereas the order of C_{2-4} paraffins selectivity completely reverses, which verifies this point of view.

***Operando* DRIFT study**. The *operando* diffuse reflectance infrared Fourier transform spectroscopy (DRIFTS) of CO_2 hydrogenation over $ZnAlO_x$ at 593 K and 0.1 MPa are explored. It is obvious from Supplementary Fig. 12 that absorbed surface formate species were first formed, then, absorbed surface methoxy species were generated by hydrogenation of formate species. As presented in Fig. 5, compared to DRIFTS of CO_2 hydrogenation over $ZnAlO_x$, the bands for surface formate (1620, 1375 and 2910 cm^{-1}) and methoxy (2940 and 2840 cm^{-1}) species[35,36] over $ZnAlO_x$&H-ZSM-5 are sharply weakened, which suggests that these active surface species over $ZnAlO_x$ were converted by H-ZSM-5. Combined the catalytic results in Fig. 1a with DRIFTS results discussed above, we propose a mechanism for CO_2 hydrogenation to aromatics over $ZnAlO_x$&H-ZSM-5. First, surface formate species on $ZnAlO_x$ was hydrogenated to form surface methoxy species; then, intermediates including MeOH and DME produced from the dissociation of methoxy species were spread to H-ZSM-5 to synthesize olefins intermediates; finally, transformation of olefins to aromatics consecutively take place in the micropores of H-ZSM-5. Furthermore, compared to CO_2 hydrogenation over $ZnAlO_x$, CO hydrogenation generates much less surface formate species. That is to say, more active metal species sites of $ZnAlO_x$ are utilized to activate H_2 during CO hydrogenation, so that higher C_{2-4} paraffins but lower aromatics are obtained in Supplementary Figure 5 because hydrogenation reactions of intermediates like olefins are enhanced. From Supplementary Fig. 13,

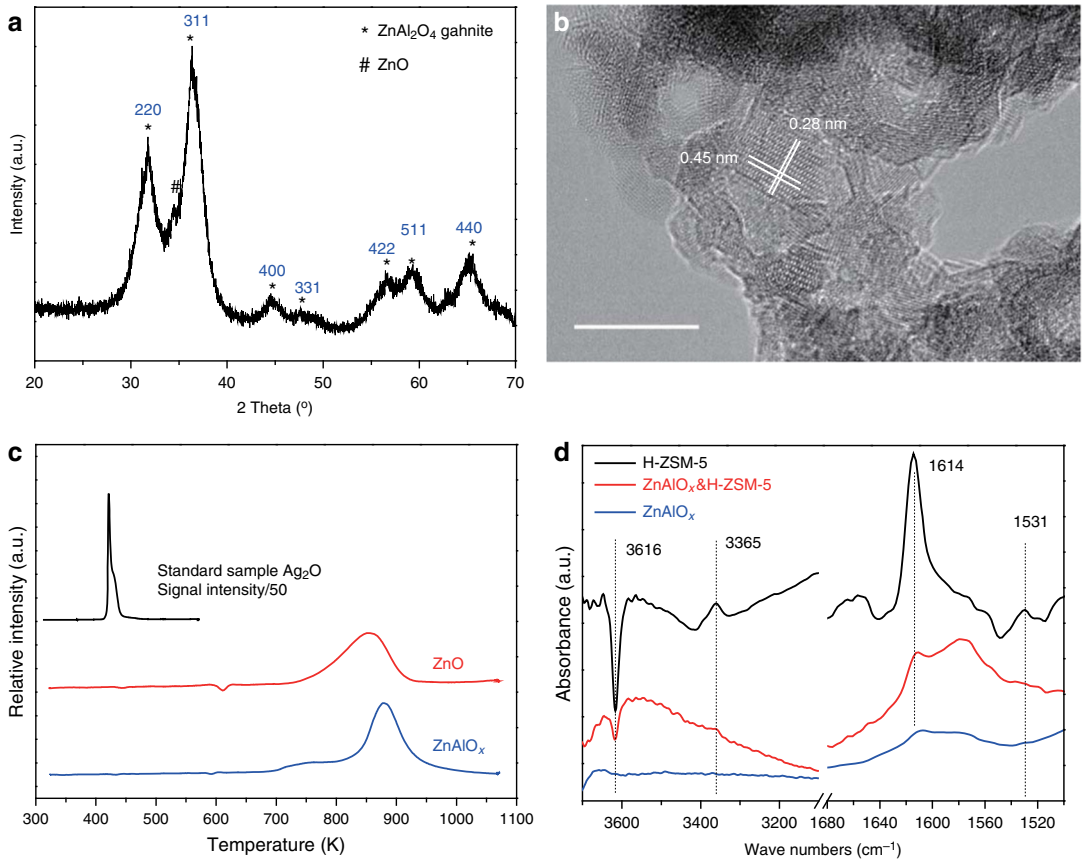

Fig. 4 Structural characterization of various catalysts. **a** X-ray diffraction patterns (XRD) of $ZnAlO_x$. **b** High-resolution transmission electron microscopy (TEM) image of $ZnAlO_x$. Scale bar: 10 nm. **c** H_2-TPR profiles. The relative intensity was normalized by weight. The relative intensity of the standard sample Ag_2O was divided by 50. **d** FTIR subtraction spectra relative to adsorption of DTBPy

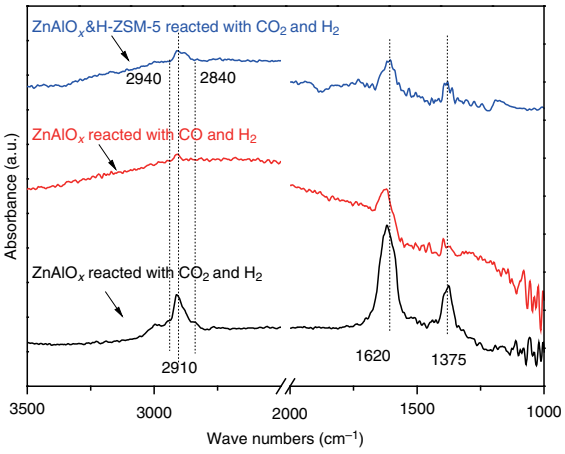

Fig. 5 *Operando* DRIFT spectra over various catalysts. Conditions: 593 K, 0.1 MPa. CO_2&H_2 refers to the mixed gas of $H_2/CO_2/Ar = 3/1/0.2$; CO&H_2 refers to the mixed gas of $H_2/CO/Ar = 3/1/0.2$

we believe that CO_2 hydrogenation cannot proceed over H-ZSM-5. Some evidences were put forward by Jiao et al.[14,17,20] to support the ketene intermediate mechanism for STO or STA reactions over oxides/zeolites composite catalysts, however, we consider that this mechanism does not work in CO_2 hydrogenation over $ZnAlO_x$&H-ZSM-5 due to very low concentration of CO in the reaction process.

In summary, composite catalyst of $ZnAlO_x$ with a nano-scaled spinel structure and H-ZSM-5 exhibits an excellent performance for CO_2 hydrogenation to aromatics. The selectivity of aromatics (excluding CO) reaches as high as 73.9% with 9.1% CO_2 conversion and 0.4% CH_4 selectivity. Increasing H_2/CO_2 ratio or introducing CO can effectively suppress RWGS reaction without obviously weakening aromatization. The composite catalyst containing Si-H-ZSM-5 presents higher *p*-xylene, ethylene and propylene selectivity. It is not zinc metal but Zn^{2+} in $ZnAlO_x$ activates CO_2 hydrogenation. The shield of the external Brønsted acid of H-ZSM-5 by $ZnAlO_x$ is beneficial to aromatization. MeOH, DME and olefins are acted as reaction intermediates. CO_2 hydrogenation over $ZnAlO_x$&H-ZSM-5 shows much higher aromatics selectivity than CO hydrogenation because the former reaction generates more formate species on $ZnAlO_x$ surface so that less metal species sites are left for hydrogenation of unsaturated intermediates like olefins. $ZnAlO_x$&H-ZSM-5 suggests a promising application in manufacturing aromatics from CO_2 and H_2.

Methods

Catalyst preparation. $ZnAlO_x$ oxide was prepared by a conventional co-precipitation method. Typically, solution A was made by 59.5 g $Zn(NO_3)_2$ $6H_2O$ and 75.0 g $Al(NO_3)_3$ $9H_2O$ dissolved in 150 ml deionized water and solution B was prepared by 23.5 g $(NH_4)_2CO_3$ dissolved in 150 ml deionized water. Solutions A and B were dividedly added into one beaker by two peristaltic pumps with constant pH of 7.1–7.3 at 343 K under continuous stirring for 0.5 h, then followed by aging for 3 h at the same temperature. After filtered and washed by 200 ml deionized water for three times, the obtained mixture was dried at 373 K overnight and then calcined at 773 K for 4 h.

Commercial Na-ZSM-5 zeolite was supplied from Zhongke New Catalytic Technology Company, China. Na-ZSM-5 zeolites were transformed into NH_4-ZSM-5 by exchanging 50 g Na-ZSM-5 with 0.5 l NH_4NO_3 (1 mol l^{-1}) aqueous solution at 353 K for 2 h, followed by filtration and washing with deionized water.

After repeating the exchanging process for three times, the resultant samples were dried overnight at 373 K, followed by calcination at 823 K for another 4 h in air to obtain the H-ZSM-5 zeolite.

Si-H-ZSM-5 zeolite was prepared by tetraethoxysilane (TEOS) modification. In brief, an organic solution was firstly made by 11.5 g TEOS mixed with 5 ml cyclohexane; then 10.0 g H-ZSM-5 was added into this solution, impregnated for 24 h at room temperature; after that, organic solvent was removed by evaporation at 353 K and the resultant powder was dried overnight at 373 K, followed by calcination at 823 K for another 4 h in air. After repeating the procedure above for twice, the Si-H-ZSM-5 was obtained.

The composite catalysts were typically prepared by physical mixing. Unless specially stated, the weight ratio of oxides and zeolites was 1:1. For preparation of the composite catalyst $ZnAlO_x$&H-ZSM-5, $ZnAlO_x$ oxide and H-ZSM-5 zeolite were grinded in an agate mortar for 4 min, pressed under 40 MPa and granulated into the required size in the range of 0.4–0.8 mm.

Catalytic tests. Catalytic reaction experiments in Fig.1 and Supplementary Figure 2 and 3 were performed in a 16-channel continuous flow fixed-bed stainless steel reactor (from Yashentech Corporation, Shanghai, China) with an 8.3 mm inner diameter for each channel. The inlet gas flow and composition along with the reaction temperature and pressure for each channel were identical. All the reaction products were kept in the gas phase and analyzed online by two gas chromatographs (Aglient 7890A) equipped with a HP-PLOT/Q capillary column connected to a flame ionization detector (FID) and a TDX-1 column (produced from DICP) connected to a thermal conductivity detector (TCD). CH_4 was taken as a reference bridge between FID and TCD. Ar was used as an inner standard. The CO_2 conversion and the CO selectivity, hydrocarbons (C_nH_m), MeOH and DME selectivity among the carbon products without CO (including C_nH_m, MeOH and DME) were calculated with the followed equations.

$$CO_2\ \text{conversion} = (CO_{2in} - CO_{2out})/(CO_{2in}) \times 100\% \quad (1)$$

CO_{2in}: moles of CO_2 at the inlet; CO_{2out}: moles of CO_2 at the outlet;

$$\text{CO selectivity} = CO_{out}/(CO_{2in} - CO_{2out}) \times 100\% \quad (2)$$

CO_{out}: moles of CO at the outlet;

$$C_nH_m\ \text{selectivity} = N_{CnHm}/(\text{total carbon atoms of products detected by FID}) \times 100\%$$

$$\text{MeOH selectivity} = N_{MeOH}/(\text{total carbon atoms of products detected by FID}) \times 100\%$$

$$\text{DME selectivity} = N_{DME}/(\text{total carbon atoms of products detected by FID}) \times 100\%$$

N_{CnHm}: carbon atoms number of C_nH_m; N_{Me6OH}: carbon atoms number of MeOH; N_{DME}: carbon atoms number of DME.

Other catalytic reaction experiments were performed in a typical fixed-bed stainless steel reactor with 8 mm inner diameter. All products were analyzed online by two tandem gas chromatographs. One is Agilent 7890A equipped with a HP-PLOT/Q capillary column connected to FID and a TDX-1 column connected to TCD. The other one is Agilent 6890N equipped with a HP-FFAP capillary column connected to FID and a Porapak Q column connected to TCD. The detailed analysis for aromatics such as ethylbenzene, *p*-xylene, *m*-xylene and *o*-xylene is dependent on HP-FFAP capillary column.

Data availability. The data supporting the findings of this study are available within the article and its Supplementary Information files. All other relevant source data are available from the corresponding author upon reasonable request.

Received: 3 May 2018 Accepted: 31 July 2018
Published online: 27 August 2018

References

1. Olah, G. A., Goeppert, A. & Prakash, G. S. Chemical recycling of carbon dioxide to methanol and dimethyl ether: from greenhouse gas to renewable, environmentally carbon neutral fuels and synthetic hydrocarbons. *J. Org. Chem.* **74**, 487–498 (2009).
2. Dorner, R. W., Hardy, D. R., Williams, F. W. & Willauer, H. D. Heterogeneous catalytic CO_2 conversion to value-added hydrocarbons. *Energy Environ. Sci.* **3**, 884–890 (2010).
3. Aresta, M., Dibenedetto, A. & Angelini, A. Catalysis for the valorization of exhaust carbon: from CO_2 to chemicals, materials, and fuels technological use of CO_2. *Chem. Rev.* **114**, 1709–1742 (2014).
4. Porosoff, M. D., Yan, B. & Chen, J. G. Catalytic reduction of CO_2 by H_2 for synthesis of CO, methanol and hydrocarbons: challenges and opportunities. *Energy Environ. Sci.* **9**, 62–73 (2016).
5. Centi, G., Quadrelli, E. A. & Perathoner, S. Catalysis for CO_2 conversion: a key technology for rapid introduction of renewable energy in the value chain of chemical industries. *Energy Environ. Sci.* **6**, 1711–1731 (2013).
6. Wang, W., Wang, S., Ma, X. & Gong, J. Recent advances in catalytic hydrogenation of carbon dioxide. *Chem. Soc. Rev.* **40**, 3703–3727 (2011).
7. Saravanan, K., Ham, H., Tsubaki, N. & Bae, J. W. Recent progress for direct synthesis of dimethyl ether from syngas on the heterogeneous bifunctional hybrid catalysts. *Appl. Catal. B* **217**, 494–522 (2017).
8. Montoya, J. H., Peterson, A. A. & Nørskov, J. K. Insights into C-C coupling in CO_2 electroreduction on copper electrodes. *Chem.Cat.Chem.* **5**, 737–742 (2013).
9. Benson, E. E., Kubiak, C. P., Sathrum, A. J. & Smieja, J. M. Electrocatalytic and homogeneous approaches to conversion of CO_2 to liquid fuels. *Chem. Soc. Rev.* **38**, 89–99 (2009).
10. Friedel, R. A. & Anderson, R. B. Composition of synthetic liquid fuels. I. product distribution and analysis of C_5-C_8 paraffin isomers from cobalt catalyst. *J. Am. Chem. Soc.* **72**, 1212–1215 (1950).
11. Puskas, I. & Hurlbut, R. S. Comments about the causes of deviations from the Anderson–Schulz–Flory distribution of the Fischer–Tropsch reaction products. *Catal. Today* **84**, 99–109 (2003).
12. Torres Galvis, H. M. & de Jong, K. P. Catalysts for production of lower olefins from synthesis gas: a review. *ACS Catal.* **3**, 2130–2149 (2013).
13. Rodemerck, U. et al. Catalyst development for CO_2 hydrogenation to fuels. *Chem.Cat.Chem.* **5**, 1948–1955 (2013).
14. Jiao, F. et al. Selective conversion of syngas to light olefins. *Science* **351**, 1065–1068 (2016).
15. Cheng, K. et al. Direct and highly selective conversion of synthesis gas into lower olefins: design of a bifunctional catalyst combining methanol synthesis and carbon-carbon coupling. *Angew. Chem. Int. Ed.* **55**, 4725–4728 (2016).
16. Zhu, Y. et al. Role of manganese oxide in syngas conversion to light olefins. *ACS Catal.* **7**, 2800–2804 (2017).
17. Jiao, F. et al. Shape-selective zeolites promote ethylene formation from syngas via a ketene intermediate. *Angew. Chem. Int. Ed.* **57**, 4692–4696 (2018).
18. Zhao, B. et al. Direct transformation of syngas to aromatics over Na-Zn-Fe $_5$ C_2 and hierarchical HZSM-5 tandem catalysts. *Chem.* **3**, 323–333 (2017).
19. Cheng, K. et al. Bifunctional catalysts for one-step conversion of syngas into aromatics with excellent selectivity and stability. *Chem.* **3**, 334–347 (2017).
20. Yang, J., Pan, X., Jiao, F., Li, J. & Bao, X. Direct conversion of syngas to aromatics. *Chem. Commun.* **53**, 11146–11149 (2017).
21. Gao, P. et al. Direct production of lower olefins from CO_2 conversion via bifunctional catalysis. *ACS Catal.* **8**, 571–578 (2017).
22. Liu, X. et al. Selective transformation of carbon dioxide into lower olefins with a bifunctional catalyst composed of $ZnGa_2O_4$ and SAPO-34. *Chem. Commun.* **54**, 140–143 (2018).
23. Li, Z. et al. Highly selective conversion of carbon dioxide to lower olefins. *ACS Catal.* **7**, 8544–8548 (2017).
24. Gao, P. et al. Direct conversion of CO_2 into liquid fuels with high selectivity over a bifunctional catalyst. *Nat. Chem.* **9**, 1019–1024 (2017).
25. Wei, J. et al. Directly converting CO_2 into a gasoline fuel. *Nat. Commun.* **8**, 15174 (2017).
26. Senger, S. & Radom, L. Zeolites as transition-metal-free hydrogenation catalysts: a theoretical mechanistic study. *J. Am. Chem. Soc.* **122**, 2613–2620 (2000).
27. Kanai, J., Martens, J. A. & Jacobs, P. A. On the nature of the active sites for ethylene hydrogenation in metal-free zeolites. *J. Catal.* **133**, 527–543 (1992).
28. Chen, X. Y., Ma, C., Zhang, Z. J. & Wang, B. N. Ultrafine gahnite ($ZnAl_2O_4$) nanocrystals: Hydrothermal synthesis and photoluminescent properties. *Mater. Sci. Eng. B.* **151**, 224–230 (2008).
29. Wang, J. et al. Partial hydrogenation of benzene to cyclohexene on a Ru–Zn/m-ZrO_2 nanocomposite catalyst. *Appl. Catal. A* **272**, 29–36 (2004).
30. Kuld, S. et al. Quantifying the promotion of Cu catalysts by ZnO for methanol synthesis. *Science* **352**, 969–974 (2016).
31. Valenzuela, M. A. et al. Effects of hydrogen at high temperature on $ZnAl_2O_4$ and Sn-$ZnAl_2O_4$. *J. Therm. Anal.* **44**, 639–653 (1995).

32. Behrens, M. et al. The active site of methanol synthesis over Cu/ZnO/Al_2O_3 industrial catalysts. *Science* **336**, 893–897 (2012).
33. Kattel, S., Ramirez, P. J., Chen, J. G., Rodriguez, J. A. & Liu, P. Active sites for CO_2 hydrogenation to methanol on Cu/ZnO catalysts. *Science* **355**, 1296–1299 (2017).
34. Ungureanu, A., Hoang, T. V., Trong On, D., Dumitriu, E. & Kaliaguine, S. An investigation of the acid properties of UL-ZSM-5 by FTIR of adsorbed 2,6-ditertbutylpyridine and aromatic transalkylation test reaction. *Appl. Catal. A.* **294**, 92–105 (2005)..
35. Mierczynski, P. et al. Cu/$Zn_xAl_yO_z$ supported catalysts (ZnO: $Al_2O_3 = 1, 2, 4$) for methanol synthesis. *Catal. Today* **176**, 21–27 (2011).
36. Le Peltier, F., Chaumette, P., Saussey, J., Bettahar, M. M. & Lavalley, J. C. In situ FT-IR and kinetic study of methanol synthesis from CO_2/H_2 over $ZnAl_2O_4$ and Cu–$ZnAl_2O_4$ catalysts. *J. Mol. Catal. A.* **132**, 91–100 (1998).

Acknowledgements

We acknowledge the financial support from the National Natural Science Foundation of China (grant no. 21606224). We thank Nan Zheng, Yanli He, Qike Jiang, Nana Yan and Peng Tian for their assistance in the experiments.

Author contributions

Y.N., who made the initial discovery, designed and conducted the experiments and wrote the manuscript. Z.C. and Y.F. conducted the experiments. Y.L. discussed the results. W.Z. and Z.L. supervised the experiments and discussed the results.

Additional information

Supplementary Information accompanies this paper at https://doi.org/10.1038/s41467-018-05880-4.

Competing interests: The authors declare no competing interests.

Reprints and permission information is available online at http://npg.nature.com/reprintsandpermissions/

Publisher's note: Springer Nature remains neutral with regard to jurisdictional claims in published maps and institutional affiliations.